Economic Analysis of a 1.5-MW-Class HTS Synchronous Machine Considering Various Commercial 2G CC Tapes

Ji Hyung Kim, Thanh Dung Le, Do Jin Kim, Chang-Jin Boo, Young-Sik Jo, Yong Soo Yoon, Kyung Yong Yoon, and Ho Min Kim

***Abstract*—We present the comparative design results of a 1.5-MW-class high-temperature superconducting synchronous machine (HTSSM) by considering various commercial 2G coated conductors (CCs). We focus on the estimation of economic factors to manufacture a more cost-effective HTSSM. A key design issue in HTSSM development is the adoption of superconducting wire among various types of recent commercial 2G CC tapes with different dimensions, critical current performance, and cost–performance ratio that affect the HTSSM performance, thermal losses, and CC tape-length usage. Therefore, we first perform the electromagnetic and thermal design of a 1.5-MW-class HTSSM considering three types of 2G CC tapes. Then, we present the comparative analysis results related to economic factors.**

***Index Terms*—Cooling expense, cost–performance (C-P) ratio, HTS synchronous machine, 2G coated conductors.**

I. Introduction

HIGH-TEMPERATURE superconducting synchronous machines (HTSSMs) are currently attracting attention in the marine-propulsion market as a good alternative to conventional machines in the next generation of electrical marine-propulsion system. They have many advantages, specifically when applied to a ship propulsion system, namely, compact volume and lighter weight, higher efficiency both at rated and low loads, low noise and vibration, and higher transient stability [1], which can overcome the limitations of conventional technology. However, despite these advantages, the high manufacturing cost of HTSSM remains the biggest obstacle in terms of economic, mechanical, thermal, and stability factors in the commercialization of HTS rotating machines. Among these factors, fabrication expenses of the rotor field coil employing costly superconducting wires and cooling expenses to cool the rotor occupy the largest proportion in the manufacturing cost component. Therefore, the economic feasibility of HTSSM depends not only on a low cost-performance (C-P) ratio but also on the HTS wire length, in addition to the initial investment in cryogenic cryocooler and cryogen cost [2]–[5].

This paper focuses on a comparative design that considers the economic factor of various commercial 2G coated-conductor (CC) tapes for a 1.5-MW-class HTSSM for various electric marine propulsion systems, such as the contra-rotating propeller (CRP) and podded propulsion systems. First, the electromagnetic and thermal designs were performed by considering three types of 2G CC tapes to analyze the HTSSM performance and thermal losses. Then, we estimated the CC tape cost to fabricate the HTS field coil and the cooling expenses for the cooling system. Finally, comparative analyses are presented to adopt the acceptable commercial 2G CC tapes that can minimize the manufacturing cost.

II. Electromagnetic Design and Analysis

A. Consideration of Commercial 2G CCs

Three types of commercialized REBCO CC tapes have been produced by SuperPower Inc. (SPI), which are already considered in electromagnetic designs of a 1.5 MW-class HTSSM. They are classified as surround copper stabilizer (SCS) 4050, 6050, and 12050-advanced pinning (AP) models. Various significant specifications of these tapes are listed in Table I.

We used specific values in this design, highlighted in bold in Table I [6]. The windings that used these three tape types selected in this research have the same thickness of 0.23 mm, including the electrical insulating layer, and widths of 4, 6, and 12 mm (Fig. 1). The machine-operating environment was assumed to be at 30 K cooling temperature and 2 T magnetic field perpendicularly applied to the tape (B_p) to establish the critical current (I_c) values. The I_c values were determined from [7], which showed the lift-factor properties of SCS-AP models of SPI under various external fields and temperatures. The lift-factor value, defined as the ratio of I_c at a given operating temperature and applied magnetic field to I_c at 77 K, at zero-field conditions (i.e., without an externally applied field) is approximately three under the operating environment [8], meaning that the I_c performance of the SCS models at 30 K and

Manuscript received October 20, 2015; accepted January 14, 2016. Date of publication January 25, 2016; date of current version May 6, 2016. This work was supported by the Ministry of Trade, Industry, and Energy and the Korea Institute for Advancement of Technology through the Promoting Regional Specialized Industry Grant R0003882.

J. H. Kim, T. D. Le, D. J. Kim, and H. M. Kim are with the Department of Electrical Engineering, Jeju National University, Jeju 63243, Korea (e-mail: hmkim@jejunu.ac.kr).

C.-J. Boo is with the Department of Electrical Engineering and Energy, Jeju International University, Jeju 63309, Korea.

Y.-S. Jo is with the Korea Electrotechnology Research Institute, Changwon 51543, Korea.

Y. S. Yoon is with the Department of Electrical Engineering, Shin Ansan University, Ansan 15435, Korea.

K. Y. Yoon is with the Department of Electrical and Electronic Engineering, Yonsei University, Seoul 03722, Korea.

Color versions of one or more of the figures in this paper are available online at http://ieeexplore.ieee.org.

Digital Object Identifier 10.1109/TASC.2016.2521408

TABLE I
MAJOR SPECIFICATIONS FOR COMMERCIAL 2G CC TAPES FROM SPI

Items	Model 1 (SCS4050)	Model 2 (SCS6050)	Model 3 (SCS12050)
Conductor type	(RE) BCO CC		
Width [mm]	4	6	12
Thickness [mm]	**0.1**–0.18		
T_{re} [μm]	1–2 (in 2014)		
T_s [μm]	**40** [#], 10-120 [##] (both sides)		
T_t [μm]	**50**, 100		
Min. I_c [A] [†]	100	150	300
S_t [MPa]/S_s [%] [†]	>550/> 0.5 @ 40 μm Cu, 77 K		
Substrate type	Hastelloy C276 (125 μΩ·cm)		
Stabilizer type	Copper		
Unit length [m]	100–**300** (in 2014)		
Joint resistance [nΩ]	<20		
I_c uniformity [%] [¥]	<10 (in 2014)		

T_{re}: REBCO thickness, T_s: Stabilizer thickness, T_t: Substrate thickness, S_t: Critical tensile strength/strain, [#]: standard product, [##]: special order product, [†]: @77 K, self-field, [¥]: Standard deviation

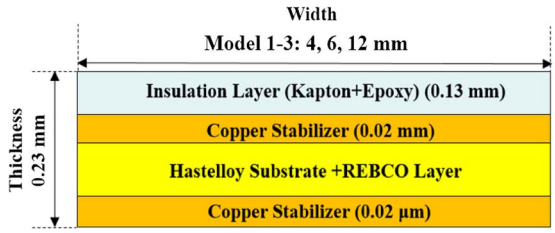

Fig. 1. Basic structure of the 2G CC tape with electrical insulating layer.

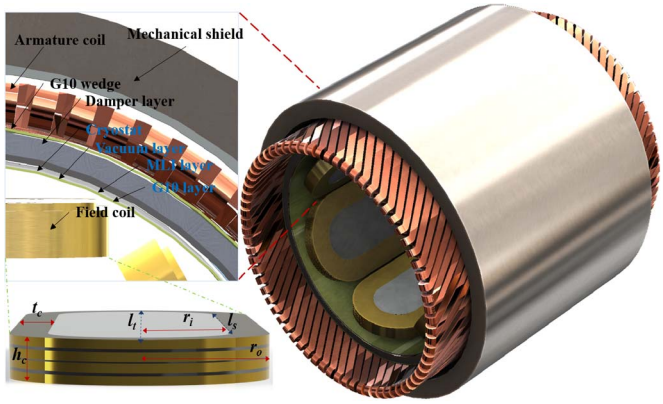

Fig. 2. Conceptual schematic of a 1.5-MW-class HTSSM.

2 T is almost three times of that at 77 K in zero-field condition. I_c for each cases was finally estimated to be from 300 to 900 A using the lift-factor characteristics in [7].

B. Electromagnetic Structure Design

Fig. 2 shows a conceptual design of a 1.5 MW-class HTSSM, and Table II lists the design parameters of the three models for 3D finite-element method (FEM) simulations. The three machines were designed to generate 1.416 MW power with phase back electromotive force (EMF) of 1873 $V_{\rm rms}$ and 252 $A_{\rm rms}$ phase current under rated operation. Moreover, to prevent loss of synchronism against load fluctuation in propulsion application, we designed the HTSSM to have a small output power margin and generate 1.5 MW maximum power by increasing the field current supplied from an inverter drive system from

TABLE II
DESIGN PARAMETER SPECIFICATIONS OF A 1.5-MW-CLASS HTSSM

Parameters	Model 1 (SCS405)	Model 2 (SCS605)	Model 3 (SCS1205)
Rated/max. power [MW]	1.42/1.5		
Rated rotating speed [rpm]	200		
Rotor pole number	6		
Rated/max. stator current density [A/mm^2]	3/3.18		
Stator coil number per slot/phase	8/192		
Physical/electromagnetic air-gap length [mm]	2/63		
Rotor outer diameter [mm]	834		
Rotor inner diameter [mm]	696/684	700/688	707/681
Stator outer diameter [mm]	1296		
Stator inner diameter [mm]	964		

252 to 267 $A_{\rm rms}$. In all models, an electromagnetic air-gap size of 63 mm was fixed to obtain the machine output power and to estimate the required CC tape length under identical design conditions.

To stably operate the HTS field coil, we set the maximum operating current $(I_{\rm op})$ values to a margin of approximately 70% of I_c to consider I_c degradation occurring after windings of the racetrack-type coil and electromagnetic disturbances in steady and transient operations [9]. This margin is defined by the $I_{\rm op}$ to I_c ratio $(I_{\rm op}/I_c)$. The closer this ratio approaches 100% in the HTS field-coil operating condition, the more possible quench can be increased.

C. 3D FEM Analysis

From [10], to minimize the required CC tape length that generates the magneto-motive force (MMF) at specific ampere-turns for a 1.5 MW output power rating and easily build the field-coil structure, we chose a rectangular-type HTS field-coil shape. Moreover, setting the inner radius of the field coil (r_i) is important in the coil-shape optimization relative to the output power and HTS field-coil performance [10]–[12]. We conclude that as r_i increases, the machine back EMF is enhanced, and B_p increases while field coil I_c decreases due to the increment in B_p. Therefore, the optimal dimensions of r_i can reduce the CC tape requirement. If the field-coil outer radius (r_o) is limited by the availability of geometric space in each pole, r_i is determined by the number of single pancake coils (SPCs). Therefore, to estimate suitable r_i dimensions considering the back EMF and I_c performance, we performed 3D-transient FEM simulations for steady-state operation considering a certain range in the number of SPCs.

Table III lists the HTS field-coil parameters of the proposed HTSSM designs. The SPC numbers for the two cases in each model were considered as suitable to estimate optimal r_i. Table III also lists the structural dimensions of the respective HTS field coil corresponding to the SPC numbers.

Table IV lists the 3D FEM analysis results for back EMF optimization in each model to estimate the CC tape length required to generate phase back EMF of 1873 $V_{\rm rms}$. These analyses were conducted according to the coil structural parameters in Table III. Among all models, those with larger r_i can well couple the flux at the air-core armature windings compared with

TABLE III
HTS FIELD COIL DESIGN PARAMETERS TO OPTIMIZE THE THREE HTSSMS

Parameters	Model 1 (SCS4050)	Model 2 (SCS6050)	Model 3 (SCS12050)
I_{op} [A]	210	315	630
J_{eo} [A/mm^2]		525	
J_{wd} [A/mm^2]		228.26	
Filling factor [%]		43.5	
Axial length l_s [mm]		635	
Number of SP coils	3/4 SPC	2/3 SPC	1/2 SPC
Total length l_t [mm]	1027/1020	1029/1022	1033/1018
Height h_c [mm]	18/26	16/24	12/28
Thickness t_c [mm]	107.64/74.29	105.57/62.56	100.28/45.54
Inner radius r_i [mm]	88.28/118.21	91.44/131	98.65/145.9
Outer radius r_o [mm]	195.92/192.5	197.01/193.5	198.93/191.4
Shape factor α [r_o / r_i]	2.22/1.63	2.15/1.48	2.02/1.31

J_e: Engineering operating current density, J_{wd}: Winding pack current density

TABLE IV
THREE-DIMENSIONAL FEM ANALYSIS RESULTS TO OPTIMIZE THE THREE HTSSM DESIGNS

Parameters	Model 1 (SCS4050)	Model 2 (SCS6050)	Model 3 (SCS12050)
HTS Synchronous Rotating Machine			
Phase back EMF [V_{rms}]	1873/1874	1874/1875	1873/1875
HTS Field Coil			
Number of SPCs	3/4 SPC	2/3 SPC	1/2 SPC
I_c [A]@30[K], B_p [T]	323/293.9	478.5/418	831/756
Lift factor ‡	3.23/2.99	3.2/2.79	2.77/2.52
I_{op} margin [I_{op}/I_c] [%]	65/71.5	65.6/75.4	75.8/83.3
Maximum B_{mag} [T]	2.88/2.97	2.92 /3.07	3.2/3.44
Maximum B_p [T]	1.75/2.03	1.78/2.26	2.27/2.65
Winding turns per pole	1404/1292	918/816	436/396
MMF [AT] (F=NI_{op})	294840 /271320	289170 /257040	274680 /249480
CC tape length [m]	18220/17412	11986/11213	5768/5536

‡: [I_c (30K, 2T)/I_c (77K, SF)]

the other models with smaller r_i. Therefore, these models can generate the target back EMF with small MMF, i.e., these models can reduce the total turns of the field coil to generate equal back EMF performance, ultimately leading to reduced CC tape requirements. The I_c values of the models with larger r_i are reduced by an increment in B_p, resulting in an increment in the I_{op} margin. For example, the total MMF in Model 3 with 2SPC was calculated to be 249480 AT (630 A × 396 turns), which was lower than 274680 AT (630 A × 436 turns) in Model 3 with 1SPC under the same phase back EMF of 1873 V_{rms}. Therefore, we realized CC tape-length savings of approximately 232 m. In contrast, I_c in Model 3 with 2SPC was approximately 9% lower than that in Model 3 with 1SPC. Thus, the I_{op} margin with 2SPC increased by as much as 7.5% compared with that with 1SPC. However, we expect that these I_{op} margin increments to be mitigated by the increase in I_c when the HTS field coils operate from 24.5 to 27 K using liquid neon (LNe) cryogen. Hence, it can match the 70% I_{op} margin, which is the initial design parameter presented in Section II-B.

Ultimately, from the comparison of the MMF values to achieve the same back EMF listed in Table IV, we decided that Model 3 with 2SPC, wound using the SCS 12050-AP type 2G CC tape, is appropriate in minimizing the winding turns and CC tape length. In addition, we concluded that designing the HTS field coil of the respective models using 4SPC, 3SPC, and 2SPC is preferable because they can minimize the required CC tape length. Further, they are thermally and mechanically designed because thinner SPCs with smaller α can be quickly and stably cooled and undergo lower mechanical stress [10].

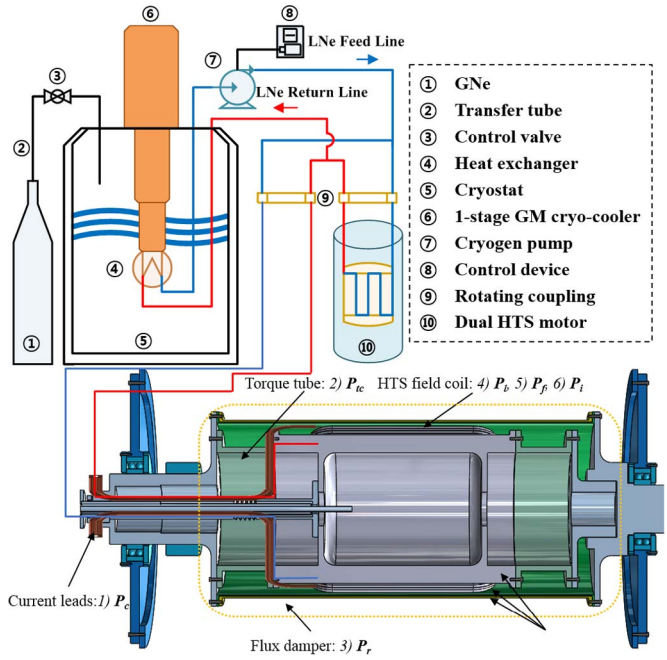

Fig. 3. Configuration of a cryogenic cooling system with conceptual schematic view of the dual HTSSM.

III. THERMAL DESIGN AND TOTAL-LOSS ESTIMATION

The cooling expense for building an external cooling system is the second dominant component in the manufacturing cost, followed by fabrication expenses of the rotor field coil [3]. Therefore, we must determine the required capacity and number of Gifford-McMahon (G-M) cryocooler and the amount of required liquid cryogen by total cooling power estimation. Fig. 3 shows the configuration of a cryogenic cooling system for an HTS CRP system, which consists of a combined dual 1.5 MW-class HTSSM. A thermosyphon conduction cooling with forced circulation and LNe were selected for field-coil cooling and cryogen for rotor cooling, respectively. LNe has been successfully applied in 1 and 5 MW-class HTSSMs manufactured by the collaboration between Korea Electrotechnology Research Institute and DOOSAN Heavy Industry in Korea [13]–[15].

The HTS field coils are cooled by LNe at 24.5 K, which flows in a circulation pipe inside the bobbin block. After the coil cooling, the heated LNe returns to the heat exchanger directly attached to a single-stage G-M cryocooler through the cooling pipe. Then, the heated LNe is cooled again. This time, the cryogen pump system can smoothly circulate the LNe. In particular, the single liquid phase of Ne is applied from 24.5 K at feed line of the cryogen pump to 27 K at return line of cryogen pump, which is called as single thermosyphon cooling method, as presented in [16].

TABLE V
COOLING LOAD ESTIMATION OF A 1.5-MW-CLASS HTSSM ROTOR

Loss [W]	Effective parameter	Model 1 (SCS405)	Model 2 (SCS605)	Model 3 (SCS12050)
P_c	I_{op} of field coil	6.27	9.41	19.52
P_{tc}	Torque tube thickness and length	4.21/4.8	4.24/4.12	5.13/4.89
P_r	Outer diameter of rotor	11.31/11.26	11.32/11.27	11.35/11.25
P_l	I_{op} of field coil and the number of joints of CC tape	0.31/0.29	0.45/0.42	0.87/0.83
P_f	I_{op} of field coil	0.13/0.12	0.77/0.72	1.79/1.72
	Critical current	0.001/0.015	0.001/0.073	0.09/1.469
Total estimated loss [W] (Average value)		22.23/22.77 (22.5)	26.19/26.02 (26.1)	38.75/39.68 (39.22)

In this paper, to estimate the cooling expense, we evaluated the total cooling load of a 1.5 MW-class HTSSM rotor by calculating the six significant thermal losses, as shown in Fig. 3, which also shows the location of each loss in the rotor. The first is the conduction loss via the current leads (P_c) and fiber reinforced plastic torque tube $(P_{\rm tc})$. The second is the radiation loss from the rotor outmost surface (P_r). The final loss is the HTS field-coil losses that include the mechanical lap joint Joule-heating (P_l), flux-flow loss (P_f), and intrinsic n-value losses (P_i) [16]–[18].

The estimations of each thermal loss for the cooling system were performed with the three models using the various 2G CC tapes listed in Table V. Further, each thermal loss in the HTSSM rotor was affected by the design parameters listed in Table V. The total cooling loads of Models 1-3 were analytically estimated from 22.23 to 39.68 W, respectively, at a 24.5-K operating temperature. Notably, thermal loss of Model 3 is the highest one compared to other models due to the major Joule-heating loss generated by high operating current of 630 A in the copper current lead. For reference, [16] presented in detail specific research on the thermal-loss estimation procedure.

Finally, we conclude that a high-capacity single-stage G-M cryocooler is sufficient to cool down the total thermal loss of a range 22.23–39.68 W based on Table V. To construct a CRP system with a combined dual 1.5 MW class HTSSM, a G-M cryocooler with a cooling capacity two times higher than the total estimated loss is required. The Sumitomo CH-110 model is a highly potential candidate for Models 1 and 2. This model has a certified cooling capacity of 34.5 W at 24.5 K. Model 3 requires a larger capacity compared with Models 1 and 2. Hence, the Cryomech AL330 model with a cooling capacity of 52.5 W at 24.5 K is sufficient. Furthermore, we estimated that the total required LNe cryogen ranges from 0.4 to 0.71 L, constantly kept at 24.5 K in the cryostat according to the different models listed in Table VI. Hence, a range of 558-996 L of GNe is required to sufficiently liquefy the estimated amount of LNe for stable operation of the HTS field coils.

IV. COMPARATIVE REVIEW

We have conducted a comparative analysis of each model considering two high-cost components that hinder the successful entry of HTSSM in the commercial market. When estimating the total cost of the required 2G CC tape to fabricate the HTS field coils, we must consider not only the unit cost or the C-P ratio but also the amount of CC tapes. Moreover, the C-P ratio of each CC tape varies with I_c performance relative to the machine operating temperature and magnetic field.

TABLE VI
COMPARISON OF FABRICATION AND COOLING EXPENSES OF THE HTS FIELD COILS FOR A 1.5-MW-CLASS HTSSM

Items	Model 1 (SCS4050)	Model 2 (SCS6050)	Model 3 (SCS12050)
Fabricating cost of HTS field coil			
CC tape length [m]	18220/17412	11986/11213	5768/5536
C–P ratio [$/kA·m]@O.C	115/125	94/108	85/93
Total cost of CC tape [$]	679424 /649293	542726 /507725	407509 /391118
Cooling expenses of HTS field coil			
Unit cost of cryocooler [$/W]	1300		
Total cost of cryocooler [$]	28897/29598	34047/33828	50370/51580
Amount of GNe [L]	279/286	329/327	487/498
Unit cost of GNe [$/L]	5		
Total cost of GNe [$]	1396/1429	1644/1634	2433/2491
Total cooling expenses [$]	30293/31028	35692/35461	52803/54071
Total investment cost [$]	709716 /680321	578418 /543186	460312 /445190

To more accurately estimate the CC tape cost, we used specific C-P ratios from the CC tape manufacturers, which were considered under operating conditions based on the 3D FEM simulation results of all models. The total costs of the required CC tapes were estimated and compared, as listed in Table VI. In the comparison, Model 3 with 2SPC requires the least budget for the winding HTS field coil of the 1.5 MW-class HTSSM. This model requires an estimated CC tape length of 5536 m at an approximate cost of $391,118.00, assuming a C-P ratio cost of $93.00 /kA · m of the SCS 12050-AP-type CC tape.

The cooling expense was also estimated using Table VI. We assumed that the cryocooler cost per watt and the GNe cost per liter are $1300.00/W and $5.00/L, respectively [19]. Model 1 with 3 and 4SPC is considered to require the least initial investment owing to its minimal cooling load of 22.23 and 22.7 W, respectively. Thus, it requires investments of $30293.00 and $31028.00 for the 3 and 4SPC cases, respectively.

Fig. 4 shows the investment-cost comparison of the HTS field coils of the six models. Model 3 with SCS 12050-AP type requires the least investment in terms of the manufacturing and cooling costs. Among all models, Model 3 is commercially acceptable for actual construction of a 1.5 MW-class HTSSM.

V. CONCLUSION

To evaluate the economic feasibility of a 1.5 MW-class HTSSM, comparative design and analyses that consider various commercially available 2G CC tapes were performed. The main purpose of this research is to estimate the material costs in fabricating and cooling the HTS field coils.

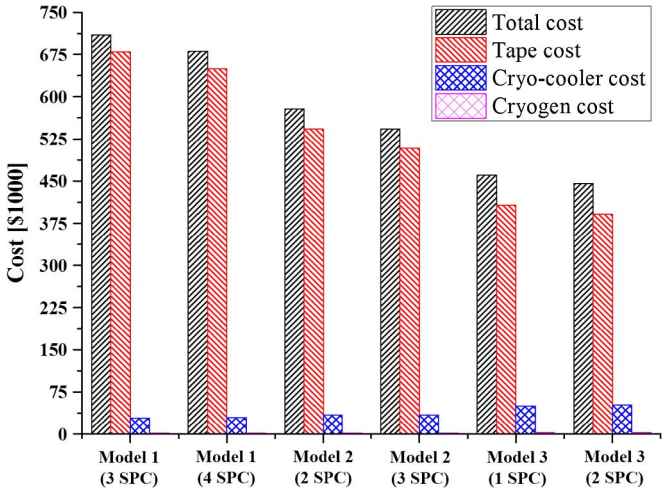

Fig. 4. Investment cost comparison for the HTS field coils of a 1.5 MW-class HTSSM in the six models.

From the comparison analyses of constructing a practical 1.5 MW-class HTSSM, Model 3 with SCS 12050-AP type, especially, using 2SPC, is found to be the best candidate owing to its economic and technical benefits in terms of manufacturing and operating the HTS field coils.

REFERENCES

[1] J. H. Kim *et al.*, "Analysis of the mechanical characteristics of a 17-MW-class high-temperature superconducting synchronous motor," *J. Supercond. Novel Magn.*, vol. 28, no. 2, pp. 1671–679, Feb. 2015.

[2] H. Karmaker, M. Ho, and D. Kulkarni, "Comparison between different design topologies for multi-megawatt direct-drive wind generators using improved second-generation high-temperature superconductors," *IEEE Trans. Appl. Supercond.*, vol. 25, no. 3, Jun. 2015, Art. no. 5201605.

[3] J. Wang *et al.*, "Comparison study of superconducting wind generators with HTS and LTS field windings," *IEEE Trans. Appl. Supercond.*, vol. 25, no. 3, Jun. 2015, Art. no. 5201806.

[4] M. D. Ainslie *et al.*, "Design and market considerations for axial flux superconducting electric machine design," *J. Phys. Conf. Ser.*, vol. 507, no. 3, Sep. 2013, Art. no. 032002.

[5] P. Masson, "Superconducting generators for large wind turbine: Design trade-off and challenges," presented at the Superconductivity Offshore Wind Turbines, Rome, Italy, 2011.

[6] 2G HTS Wire Specification Overview, Jun. 1, 2015. [Online]. Available: www.superpower-inc.com/content/wire-specification

[7] D. W. Hazelton, "2G HTS wire for demanding applications and continuous improvement plans," in *Proc. EUCAS*, Genova, Italy, Sep. 2013, pp. 1–26.

[8] V. Selvamanickam *et al.*, "The low-temperature, high-magnetic-field critical current characteristics of Zr-added (Gd, Y) $Ba_2Cu_3O_x$ superconducting tapes," *Supercond. Sci. Technol.*, vol. 25, no. 12, Oct. 2012, Art. no. 125013.

[9] S. K. Baik *et al.*, "Design considerations for 1MW class HTS synchronous motor," *IEEE Trans. Appl. Supercond.*, vol. 15, no. 2, pp. 2202–2205, Jun. 2005.

[10] J. H. Kim *et al.*, "Characteristic analysis of various structural shapes of superconducting field coils," *IEEE Trans. Appl. Supercond.*, vol. 25, no. 3, Jun. 2015, Art. no. 5201105.

[11] R. Shafaie and M. Kalantar, "Design of a 10-MW-class wind turbine HTS synchronous generator with optimized field winding," *IEEE Trans. Appl. Supercond.*, vol. 23, no. 4, Aug. 2013, Art. no. 5202307.

[12] J. J. Lee, Y.-S. Jo, J. P. Hong, and Y. K. Kwon, "Design of field coil for 100-hp-class HTS motor considering operating current," *IEEE Trans. Appl. Supercond.*, vol. 13, no. 2, pp. 2214–2216, Jun. 2003.

[13] Y. K. Kwon *et al.*, "Development of HTS motor for industrial applications at KERI & DOOSAN," in *Proc. IEEE Power Eng. Soc. Gen. Meet.*, Jan. 2006, pp. 1–8.

[14] Y. K. Kwon *et al.*, "Status of HTS motor development in Korea," in *Proc. IEEE Power Eng. Soc. Gen. Meet.*, Tampa, FL, USA, Jun. 2007, pp. 1–5.

[15] Y. K. Kwon *et al.*, "Status of HTS motor development for industrial applications at KERI & DOOSAN," *IEEE Trans. Appl. Supercond.*, vol. 17, no. 2, pp. 1587–1590, Jun. 2007.

[16] T. D. Le, "A compact integration cooling system of a combination dual 1.5-MW HTS motors for electric propulsion," presented at the European Conf. Applied Superconductivity, Lyon, France, 2015.

[17] T. D. Le *et al.*, "Thermal design of a cryogenics cooling system for a 10-MW class high-temperature superconducting rotating machine," *IEEE Trans. Appl. Supercond.*, vol. 25, no. 3, Jun. 2015, Art. no. 3800305.

[18] T. D. Le *et al.*, "Transient characteristics of current lead losses for the large scale high-temperature superconducting rotating machine," *Progr. Supercond. Cryogenics*, vol. 16, no. 4, pp. 62–65, Dec. 2014.

[19] H. Karmaker *et al.*, "High-power dense electric propulsion motor," *IEEE Trans. Ind. Appl.*, vol. 51, no. 2, pp. 1341–1347, Mar./Apr. 2015.